04.2

Plasma potential evolution in the scenarios with cryogenic pellet injection in TUMAN-3M tokamak

© A.A. Belokurov, G.I. Abdullina, L.G. Askinazi, N.A. Zhubr, V.A. Kornev, S.V. Lebedev, D.V. Razumenko, A.I. Smirnov, A.S. Tukachinskiy, D.A. Shergin, L.K. Shuvalova

Ioffe Institute, St. Petersburg, Russia
E-mail: belokurov@mail.ioffe.ru

Received June 6, 2024
Revised July 12, 2024
Accepted July 12, 2024

In TUMAN-3M tokamak the series of experiments with cryogenic hydrogen pellet injection was carried out. In these experiments the evolution of plasma potential in central and peripheral regions of plasma discharge was studied by means of heavy ion beam probe and Langmuir probe diagnostics. Measurements show that the evaporation of solid pellet in the chosen experimental set-up could initiate temporal confinement improvement (up to 2-3 ms).

Keywords: Plasma physics, tokamak, pellet injection, heavy ion beam probe, potential, radial electric field.

DOI: 10.61011/TPL.2024.11.59666.20015

The injection of pellets into tokamak plasma is one of the methods of plasma confinement control. Cryogenic fuel pellets allow for efficient delivery of large numbers of particles into the central region of a plasma. When evaporated at the periphery, both fuel and impurity pellets are capable of forming a region with strong electron and ion pressure gradients, which exert a direct influence on plasma confinement. Impurity pellets may induce controlled perturbations at the periphery of a plasma and extract (through radiation) excess energy if a plasma discharge disruption is possible.

The first experiments into the influence of pellets on plasma confinement and initiation of the transition to the H-mode (high-confinement mode) have been carried out at the TUMAN-3M tokamak in 1993 [1]. An impurity (LiD) pellet injected in the radial direction was used in these experiments. The injection of a pellet was also found to improve confinement at the T-10 tokamak [2]. A reduction in the threshold heating power required for the transition to the H-mode was observed at the DIII-D tokamak in experiments with pellet injection [3]. The injection of deuterium pellets coupled with additional plasma heating was found to induce the transition to the H-mode at the MAST and EAST tokamaks [4,5].

The evaporation of a pellet in plasma and subsequent ionization of evaporated matter induce a local perturbation of the particle source, local cooling of the ion component of plasma due to the dilution of thermal ions by colder ions from the pellet material, and a local increase in the flux of ion heat via the charge exchange channel and electron heat via the ionization channel; electron heat is also spent on radiation and heating of matter evaporated from the pellet surface. Thus, pellet evaporation leads to a local perturbation of the gradients of density and ion and electron temperatures and, as a consequence, to a perturbation of the radial electric field and the plasma potential, which may be determined according to the neoclassical theory [6]:

$$E_r = \frac{T_i}{e}\left[\frac{\partial \ln n}{\partial r} + k_T \frac{\partial \ln T_i}{\partial r}\right],$$

where n is the plasma density, T_i is the ion temperature, e is the electron charge, and k_T is the neoclassical coefficient.

The emergence of a radial electric field E_r with a large non-uniformity (the so-called shear

$$\omega_{ExB} = \left|\frac{RB_\theta}{B_T}\frac{\partial}{\partial r}\left(\frac{E_r}{RB_\theta}\right)\right|$$

with B_θ and B_T being poloidal and toroidal magnetic fields and R being the major plasma radius) contributes to the suppression of turbulence and the initiation of the transition of plasma to the H-mode [7]. This mechanism, and also the influence of the pellet-related particle source, and the effect of pellet evaporation on turbulence development have been analyzed in earlier studies [8] by numerical modeling with a transport model [8,9] and a gyrokinetic code [10].

In the present study, we report the results of direct measurements of evolution of the plasma potential in central and peripheral plasma regions in discharges with pellet injection. Measurements were performed using Langmuir probes and, for the first time at the TUMAN-3M tokamak, a heavy ion beam probe (HIBP); the principles of operation and features of the diagnostic complex at the TUMAN-3M tokamak were detailed in [11]. The obtained data may be compared to the results of numerical modeling of earlier experimental scenarios [8–10].

A pneumatic injector manufactured by PELIN [12], which allows one to launch up to four cryogenic fuel pellets with a diameter ranging from 0.6 to 1.0 mm into plasma, is currently installed at the TUMAN-3M tokamak

($R = 0.55$ m, $a = 0.22$ m, $B_T < 1$ T, $I_p < 180$ kA). Helium was used as an accelerating gas. A pellet launched by the injector propagates within a 6.3-m-long injection duct through differential pumping systems. This helps minimize the ingress of accelerating gas into plasma. The diagram of the experiment is shown in Fig. 1. Injection is performed in the tangential direction through the neutral beam injection (NBI) duct. The impact parameter of pellet injection is 54 cm; in the equatorial projection, the angle between the neutral heating beam axis and the pellet injection trajectory is 13°, and the trajectories intersect at the center of the inlet NBI duct. At pellet velocities ranging from 200 to 600 m/s, this configuration provides an opportunity to concentrate evaporation in the peripheral area ($r/a > 0.4$). The pellet velocity is set indirectly by adjusting the accelerating gas pressure (with an accuracy of approximately ±50 m/s) and determined by measuring the interval between the moments of activation of a pair of light barriers in the injector by a pellet passing through them [12].

An optical H_α/D_α line emission sensor was used to monitor the pellet evaporation in plasma; the direction pattern of this sensor is oriented along the pellet trajectory (Fig. 1). A well-defined peak in the sensor signal (the so-called pellet evaporation curve) allows one to identify the moment of entry and the time of evaporation of a pellet in plasma. The classical evaporation curve shape [13] characterized by a rapid growth within 0.2–0.5 ms and an even more rapid decline is seen in discharges. Such an evaporation curve forms when a solid pellet enters plasma. If the injection geometry, the pellet velocity, and the geometry of observation of emission of the evaporating pellet material are known, one may infer the depth of pellet penetration into plasma from the shape of the evaporation curve.

Figures 2, *a*, *b* and 3 present the examples of evolution of discharge parameters at the TUMAN-3M tokamak with pellet injection. The evolution of plasma potential, local electron density and temperature at the periphery (in the shadow of the limiter in the immediate vicinity of the last closed flux surface) in the discharges in Figs. 2, *a* and *b* was examined using a Langmuir probe. In the discharge in Fig. 3, the evolution of plasma potential was investigated with HIBP at minor radius $r/a = 0.7$.

In discharge 24040908 (Fig. 2, *a*), a pellet with an initial diameter of 0.7 mm entered plasma at 68.3 ms with a velocity of approximately 480 m/s and was evaporated completely at relative minor radius $r/a = 0.74$. In discharge 24041711 (Fig. 2, *b*), a pellet with an initial diameter of 0.6 mm entered plasma at 60.2 ms with a velocity of approximately 400 m/s and was evaporated completely at $r/a = 0.71$. In discharge 24041716 (Fig. 3), a pellet entered plasma at 63 ms. This pellet had an approximate velocity of 300 m/s and an initial diameter of 0.8 mm and penetrated plasma to a radius of $r/a = 0.77$. The size and velocity of pellets were determined in such a way that their evaporation was confined to the periphery of the plasma and, if possible, did not disrupt the discharge.

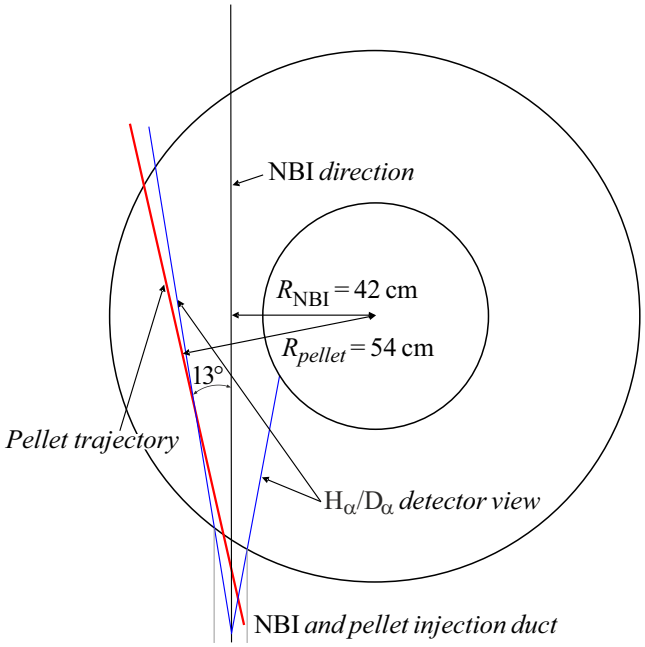

Figure 1. Diagram of the experiment on pellet injection into the TUMAN-3M tokamak in the equatorial plane. The pellet trajectory, the neutral beam injection (NBI) direction, and the field of view of H_α/D_α emission sensors, which „monitor" the process of pellet evaporation, are indicated. The impact parameters of NBI ($R_{\mathrm{NBI}} = 42$ cm) and pellet injection ($R_{pellet} = 54$ cm) are also specified.

The evolution of plasma parameters during pellet injection may be divided tentatively into three phases (Figs. 2, *a*, *b* and 3).

Phase I corresponds to unperturbed ohmic plasma prior to pellet entry with a chord-average density at the central chord of the interferometer being equal to $(1.2–1.5) \cdot 10^{19}$ m^{-3}.

Phase II includes pellet evaporation and modification of plasma profiles and parameters. The chord-average density measured along the central chord increases sharply in this phase after pellet evaporation; in the course of evaporation, a peak is observed in the signals of H_α/D_α emission sensors. This increased density is maintained at the peak level for 2–3 ms, which is accompanied by a reduction in the H_α/D_α line emission intensity at the periphery after pellet evaporation. The local density at the limiter edge decreases in Fig. 2, *a* and increases in Fig. 2, *b* relative to the value in phase I. A similar evolution is observed for the chord-average density on the peripheral chord. The results of measurements with the Langmuir probe reveal a reduction in the plasma floating potential and electron temperature in the shadow of the limiter (Figs. 2, *a* and *b*). HIBP measurements also demonstrate that the plasma potential decreases after pellet evaporation (Fig. 3). The signal from fast magnetic probes illustrates a decrease in the high-frequency part of the spectrum of magnetohydrodynamic (MHD) oscillations.

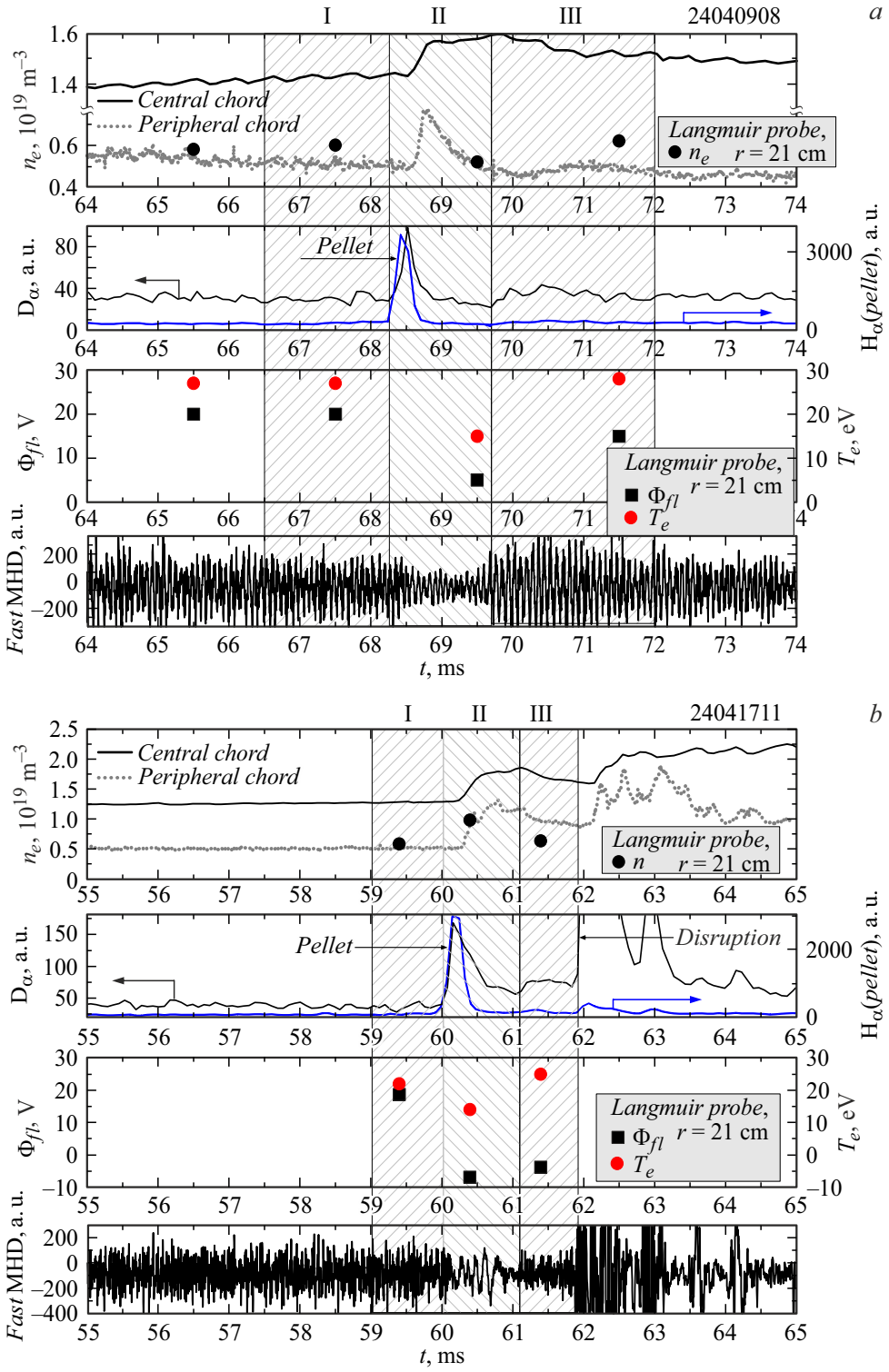

Figure 2. Injection of a cryogenic pellet into the TUMAN-3M tokamak. *a* — Measurements in a discharge with temporal confinement improvement. *b* — Measurements in a discharge without confinement improvement. From top to bottom: chord-average plasma density and local plasma density at the periphery measured with Langmuir probes; D_α line emission at the periphery (left axis) and signal from the optical sensor „looking" along the pellet trajectory (right axis); floating potential and electron temperature of plasma at the periphery measured with Langmuir probes; and signal from high-frequency MHD probes.

Phase III corresponds to the state of plasma after thermalization and dispersion of the pellet material in plasma. The chord-average density on the central chord decreases, and the intensity of high-frequency oscillations

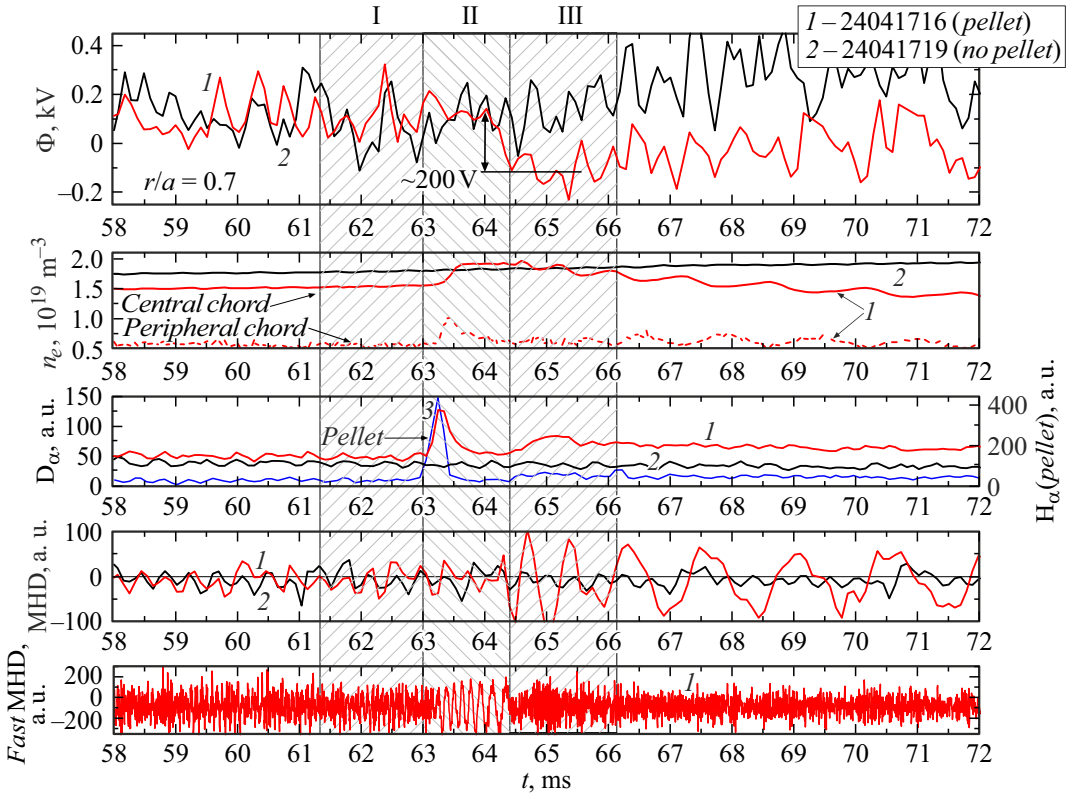

Figure 3. Evolution of the plasma potential measured using HIBP in a discharge with pellet injection (red lines *1*) and a similar discharge without a pellet (black lines *2*). From top to bottom: plasma potential at 15 cm ($r/a = 0.7$); chord-average plasma density; D_α line emission at the periphery and signal from the optical sensor „looking" along the pellet trajectory (blue lines *3*); signal from low-frequency MHD probes; and signal from high-frequency MHD probes. A color version of the figure is provided in the online version of the paper.

at fast MHD probes, the floating potential of plasma, and the electron temperature in the shadow of the limiter rise to their initial levels (corresponding to phase I). The D_α line emission signal at the periphery intensifies to a value exceeding the one observed in phase II. An increase in MHD activity with the formation of a large magnetic island and degradation of confinement with a strong modulation of the plasma potential and density at the frequency of MHD oscillations (Fig. 3) or disruption of the discharge may also be observed in phase III (Fig. 2, *b*).

The behavior of plasma parameters in Figs. 2, *a* and 3 may indicate that pellet evaporation resulted in a short-term (several milliseconds) improvement of confinement, which is characterized by the formation of a transport barrier at the periphery. The following are the signs of formation of a peripheral transport barrier: (1) reduction in local density at the periphery (outside the barrier) with a simultaneous increase in chord-average plasma density; (2) lowering of the D_α line emission intensity at the periphery; and (3) reduction in the intensity of high-frequency fluctuations, including those recorded by fast magnetic probes (this is often observed during the L–H transition at the TUMAN-3M tokamak). The formation of the transport barrier is accompanied by the generation of peripheral negative E_r, which also manifests itself in the evolution of the plasma potential toward negative values. A reduction in local electron temperature at the plasma boundary with a simultaneous increase in T_e at the center may also be indicative of the formation of a temperature transport barrier; the transport barrier at T_e at the TUMAN-3M tokamak is normally located deeper in plasma than the density barrier [14].

The HIBP measurement results (Fig. 3) demonstrate that the potential decreases approximately by 200 V relative to the reference discharge. This provides an opportunity to estimate the radial electric field variation as $E_r = \Delta\Phi/(a - r)$, which corresponds to about 3 kV/m. The obtained estimate exceeds the values found in modeling in [8,10]. This discrepancy warrants a more thorough study with direct measurements of E_r in the pellet evaporation region.

The reduction in local density at the plasma periphery in discharges 24040908 (Fig. 2, *a*) and 24041716 (Fig. 3) may justify the association of the observed phenomenon with confinement modification instead of just the influence of locally varying density and temperature gradients on electric field

$$E_r = \frac{T_i}{e}\left[\frac{\partial \ln n}{\partial r} + k_T \frac{\partial \ln T_i}{\partial r}\right].$$

The scenario illustrated in Fig. 2, *b* provides an example of pellet evaporation that does not result in a temporal

confinement improvement. Although the potential and the electron temperature decrease in this scenario, the plasma density at the periphery (i.e., outside the transport barrier) increases after pellet evaporation (in contrast to the scenario presented in Fig. 2, *a*). In addition, the H_α/D_α line emission intensity does not decrease at the periphery in this case. The reduction in plasma potential and electron temperature without any improvement of confinement may be regarded as a consequence of local plasma cooling and local perturbation of the particle and heat source, which may lead to perturbation of profiles with the formation of steeper density and temperature gradients (see [8]). The suppression of fluctuations, which is also observed in this scenario, may be associated with a significant change in the collisionality in plasma in the region of pellet evaporation (due to rapid local cooling and an increase in the plasma density during pellet evaporation) instead of the suppression of turbulence due to the shear of plasma rotation. As a result, the conditions for turbulence build-up are not satisfied prior to the thermalization of pellet material in the discussed region (see [10] for details).

Experiments with pellet injection, which were the first where the evolution of plasma potential during pellet evaporation was examined with HIBP, were carried out at the TUMAN-3N tokamak. Pellet evaporation shifts the potential toward more negative values and leads to suppression of fluctuations, but the latter change may be associated with both a short-term improvement of plasma confinement and a temporary lapse in fulfillment of requirements for the build-up of the dominant turbulent mode due to local cooling and an increase in collisionality.

It may be assumed that the background plasma density needs to be increased in order to observe a self-sustaining transition to the improved confinement mode, since the particle source size in the current configuration does not ensure the existence of a stationary H-mode [8,9]. It is also necessary to use smaller pellets that do not induce plasma disruption. This should enable the use of pellet injection in scenarios with higher plasma densities and in scenarios with simultaneous injection of neutral atoms and a pellet, which allow for a stable transition to the H-mode initiated by pellet evaporation [8].

Funding

The operation of standard diagnostics of the TUMAN-3M tokamak is supported under state contract FFUG-2024-0028 of the Ioffe Institute. Experiments with pellet injection were supported under state contract 0034-2021-0001 of the Ioffe Institute. Measurements of the plasma potential at the TUMAN-3M tokamak are performed with support from the Russian Science Foundation (project 22-12-00062).

Conflict of interest

The authors declare that they have no conflict of interest.

References

[1] L.G. Askinazi, V.E. Golant, S.V. Lebedev, L.S. Levin, V.A. Rozhansky, M. Tendler, Phys. Fluids B, **5**, 2420 (1993). DOI: 10.1063/1.860726
[2] V.G. Kapralov, V.A. Rozhanskii, K.V. Khlopenkov, Pis'ma Zh. Tekh. Fiz., **21** (6), 57 (1995) (in Russian).
[3] P. Gohil, L.R. Baylor, T.C. Jernigan, K.H. Burrell, T.N. Carlstrom, Phys. Rev. Lett., **86**, 644 (2001). DOI: 10.1103/PhysRevLett.86.644
[4] M. Valovič, L. Garzotti, C. Gurl, R. Akers, J. Harrison, C. Michael, G. Naylor, R. Scannell and the MAST Team, Nucl. Fusion, **52**, 114022 (2012). DOI: 10.1088/0029-5515/52/11/114022
[5] X.J. Yao, J.S. Hu, Y. Chen, Z. Sun, H.Q. Liu, H. Lian, S.X. Wang, Y.X. Jie, N. Shi, G.S. Xu, Q.Q. Yang, T.H. Shi, C. Zhou, Z. Xu, X. Zhu, T.F. Wang, Q. Zang, Y. Yuan, C.Z. Li, X.W. Zhen, X.Z. Gong, J. Li, G.J. Wu, X.L. Yuan and the EAST Team, Nucl. Fusion, **57**, 066002 (2017). DOI: 10.1088/1741-4326/aa665c
[6] S.P. Hirshman, D.J. Sigmar, Nucl. Fusion, **21**, 1079 (1981). DOI: 10.1088/0029-5515/21/9/003
[7] H. Biglari, P.H. Diamond, P.W. Terry, Phys. Fluids B, **2**, 1 (1990). DOI: 10.1063/1.859529
[8] A.A. Belokurov, L.G. Askinazi, L. Chôné, E.Z. Gusakov, T.P. Kiviniemi, V.A. Kornev, T. Korpilo, S.V. Krikunov, S.V. Lebedev, S. Leerink, P. Niskala, R. Rochford, A.I. Smirnov, A.S. Tukachinsky, N.A. Zhubr, Nucl. Fusion, **58**, 112007 (2018). DOI: 10.1088/1741-4326/aac4e9
[9] A.A. Belokurov, G.I. Abdullina, L.G. Askinazi, V.V. Bulanin, L. Chôné, A.D. Gurchenko, E.Z. Gusakov, T.P. Kiviniemi, V.A. Kornev, S.V. Krikunov, D.V. Kouprienko, S.I. Lashkul, S.V. Lebedev, S. Leerink, P. Niskala, A.V. Petrov, D.V. Razumenko, A.S. Tukachinsky, A.Yu. Yashin, N.A. Zhubr, Phys. Scripta, **95**, 115604 (2020). DOI: 10.1088/1402-4896/abbfcc
[10] T.P. Kiviniemi, P. Niskala, L.G. Askinazi, A.A. Belokurov, L. Chôné, A.D. Gurchenko, E.Z. Gusakov, T. Korpilo, S.V. Lebedev, S. Leerink, R. Rochford, A.S. Tukachinsky, Plasma Phys. Control. Fusion, **60**, 085010 (2018). DOI: 10.1088/1361-6587/aac917
[11] L. Askinazi, G. Abdullina, A. Belokurov, V. Kornev, S. Lebedev, D. Razumenko, D. Shergin, A. Smirnov, A. Tukachinsky, N. Zhubr, Atoms, **10**, 152 (2022). DOI: 10.3390/atoms10040152
[12] I.V. Vinyar, A.P. Umov, A.Ya. Lukin, P.V. Reznichenko, Instrum. Exp. Tech., **49** (5), 717 (2006). DOI: 10.1134/S0020441206050204.
[13] G. Pegourie, Plasma Phys. Control. Fusion, **49**, R87 (2007). DOI: 10.1088/0741-3335/49/8/R01
[14] L.G. Askinazi, V.V. Bulanin, M.I. Vildjunas, V.E. Golant, M.V. Gorokhov, V.A. Kornev, S.V. Krikunov, S.V. Lebedev, A.V. Petrov, V.V. Rozhdestvensky, A.S. Tukachinsky, N.A. Zhubr, Plasma Phys. Control. Fusion, **46**, A51 (2004). DOI: 10.1088/0741-3335/46/5A/005

Translated by D.Safin